Slip Velocity and Slip Layer Thickness in Flow of Concentrated Suspensions

FAEZEH SOLTANI,* ÜLKÜ YILMAZER

Chemical Engineering Department, Middle East Technical University, Ankara, Turkey

Received 15 September 1997; accepted 13 February 1998

ABSTRACT: The rheological characterization of highly filled suspensions consisting of a Newtonian matrix (hydroxyl-terminated polybutadiene), mixed with two different sizes of aluminum powder (30% and above by volume) and two different sizes of glass beads (50% and above by volume), was performed using a parallel disk rheometer with emphasis on the wall slip phenomenon. The effects of the solid content, particle size, type of solid particle material, and temperature on slip velocity and slip layer thickness were investigated. Suspensions of small particles of aluminum (mean diameter of 5.03 μm) did not show slip at any concentration up to the maximum packing fraction. However, suspensions of the other particles exhibited slip at the wall, at concentrations close to their maximum packing fraction. In these suspensions, the slip velocity increased linearly with the shear stress, and at constant shear stress, the slip velocity increased with increasing temperature. The slip layer thickness increased proportionally with increasing size of the particles for the glass beads. Up to a certain value of (filler content/maximum packing fraction), ϕ/ϕ_m, the slip layer thickness divided by the particle diameter, δ/D_P, was 0, but it suddenly increased and reached a value that was independent of ϕ/ϕ_m and the temperature. On average, the ratio of δ/D_P was 0.071 for aluminum and 0.037 for glass beads. © 1998 John Wiley & Sons, Inc. J Appl Polym Sci 70: 515–522, 1998

Key words: suspension; slip at the wall; slip layer thickness; suspension rheology; slip velocity

INTRODUCTION

Existing experimental and theoretical work on dilute and concentrated suspension rheology[1–4] generally emphasize the effects of shape, size and size distribution and volume fraction of particles, particle–particle and particle–matrix interactions, and matrix rheology as the major factors contributing to the complex flow behavior of suspensions. However, especially in concentrated suspensions that are filled with solids at concentrations approaching their maximum packing fraction, slip at the wall becomes the controlling factor. Slip velocity versus shear stress behavior of concentrated suspensions can be characterized over a broad shear stress range using simple shear flows.[5–8]

Slip phenomenon is the occurrence of a relative velocity between the fluid at the wall and the wall itself. For unfilled polymeric melts, the mechanism of slip is referred to as the "true slip"[9] (i.e., a discontinuity in the velocity at the wall). In concentrated suspensions, however, true slip does not occur, but rather an "apparent slip" caused by a region of higher velocity gradient adjacent to

Correspondence to: Ü. Yilmazer.
* *Present address:* Mechanical Engineering Department, Stevens Institute of Technology, Hoboken, NJ 07030.

Journal of Applied Polymer Science, Vol. 70, 515–522 (1998)
 CCC 0021-8995/98/030515-08

Table I Solid Particles' Specifications

Raw Material	Density (g cm^{-3})	Average Diameter (μm)	Volume Fraction in the Suspension [ϕ (%)]	Maximum Packing Fraction (ϕ_m)
Aluminum	2.7	5.03	30, 40, 50	0.52
Aluminum	2.7	10.4	30, 40, 50, 63	0.63
Glass beads	2.53	45.94	63	0.63
Glass beads	2.53	150.0	50, 58, 63	0.63

the wall is encountered. With concentrated suspensions, for example, the local concentration of suspended particles is lower near the wall than in the bulk. When the material is sheared, large velocity gradients are produced in this low viscosity layer, resulting in apparent slippage of the bulk fluid.[10] Apparent slip is encountered with various other fluids, including aqueous foams and emulsions.[11] The rheological data of a suspension exhibiting wall slip need to be corrected to characterize the true rheological behavior of the suspension. The classic earlier techniques for capillaries and Couette geometries were first presented by Mooney.[12] The use of torsional flows to determine wall slip behavior is fairly recent in comparison with the characterization of wall slip behavior in capillary flows.[11] The parallel disk geometry has several experimental advantages over the other geometries, such as flow regularity and ease of sample preparation, but it has the disadvantage of nonuniform shear strain in the sample. The traditional method of correcting for wall slip and obtaining the slip velocity *versus* shear stress information in parallel disk torsional flows involves experiments with multiple gap separations.[5,11]

This study is an investigation on the effects of particle size, volume fraction, and temperature on the rheological behavior of concentrated suspensions. For the first time, the effects of all of the previously described parameters on slip velocity and slip layer thickness of the suspensions, filled close to their maximum packing fraction, were investigated by using multiple gap separations in a parallel disk rheometer. Such a study has been lacking, especially in terms of particle size, type of particle material, and filler content dependence. A limited study of only the temperature effect is given in Aral and Kalyon.[13]

EXPERIMENTAL

Materials

The polymer matrix of the concentrated suspensions was (hydroxyl-terminated polybutadiene; HTPB), manufactured by Atlantic Richfield. This polymer had a specific gravity of 0.85. In the shear rate range of 0.1 and 4 s^{-1}, the shear viscosity of HTPB was found to be independent of the deformation rate. The steady shear viscosity values in this shear rate range were 8.37, 4.07, and 1.47 Pa · s at 21, 40, and 60°C, respectively.

Suspensions were prepared with solid glass spheres or aluminum spheres available from different suppliers. The maximum packing fraction, ϕ_m, of the particles were determined by measuring the weight and volume of particles in a graduated cylinder, after shaking overnight to allow the packing of the particles. The specifications and the volume fractions of the fillers, contained in the suspension, are given in Table I; size distributions are shown in Figure 1.

In the material preparation, the first stage was the mixing of HTPB with fillers. Mixing was per-

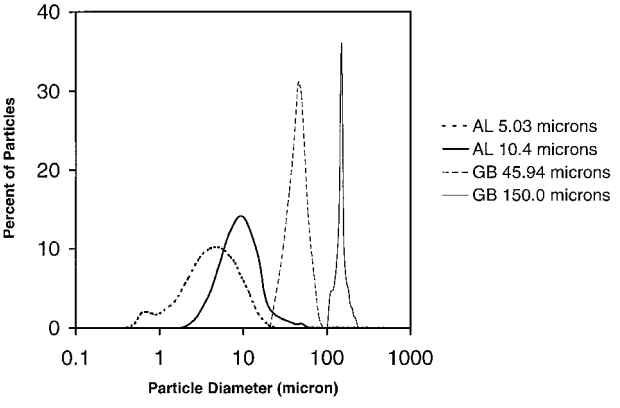

Figure 1 Size distribution of the particles used. AL, aluminum; GB, glass beads.

formed for approximately half an hour in an injector, the mouth portion of which was 4 mm in diameter. Then, the sample was subjected to vacuum. This was essential for the removal of air bubbles, which were earlier entrained into the suspension. After this, the samples were rotated until they were used to prevent settling of the particles.

Rheological Characterization

Suspension samples were characterized using a HAAKE parallel disk rheometer. The diameter of the disks used were 19.25 mm. In the computerized measurement system, the software ROT24 was used for steady shear experiments, and the resulting shear stress or torque was measured.

Torsional flow behavior of the concentrated suspensions was characterized at 21, 40, and 60°C using various gap heights in the range of 1 to 4 mm. At each experiment, a fresh sample was used, and preshearing of the sample was avoided. Data were collected by repeating the experiment for at least five independent runs, and the sample loading procedures were kept identical in each experimental run.

BACKGROUND

To determine wall slip velocity and actual shear rate in parallel disk experiments, Yoshimura and Prud'homme[11] outlined a method based on performing two sets of experiments at two gap heights and a procedure for correcting the parallel disk torsional flow data. In the parallel disk torsional flow, the apparent shear rate, $\dot{\gamma}_a$ (not corrected for slip effects) is a linear function of the radius, r, given by

$$\dot{\gamma}_a = \frac{\Omega \cdot r}{H} \tag{1}$$

where r is the radial distance from the center of the disk, H is the gap height, and Ω is the angular velocity of the rotating disk. The apparent shear rate is related to the true shear rate, $\dot{\gamma}$, and slip velocity, U_s, by the following equation:

$$\dot{\gamma}_a = \dot{\gamma}(\tau_{Z\theta}) + \frac{2U_s(\tau_{Z\theta})}{H} \tag{2}$$

Here, $\dot{\gamma}(\tau)$ and $U_s(\tau)$ (i.e., the true shear rate and slip velocity) are functions of the shear stress, τ. Shear stress at the edge of the disk, τ_R, can be determined from

$$\tau_R = \frac{T_t}{2\pi R^3}\left[3 + \frac{d \ln T_t}{d \ln \dot{\gamma}_{aR}}\right] \tag{3}$$

where T_t is the torque required to rotate the rotating disk, and $\dot{\gamma}_{aR}$ is the apparent shear rate at the edge of the disk obtained by substituting $r = R$ in eq. (1). This step is analogous to the differentiation that produces the Weissenberg–Rabinowitsch equation for flow in a capillary. The function $f = \dfrac{d \ln T_t}{d \ln \dot{\gamma}_{aR}}$ is dependent on the gap height used. Note that, for a Newtonian material, the shear stress is given by $\tau_R = \dfrac{2T_t}{\pi R^3}$, because the second term in parentheses is equal to 1. The instrument used in this study gives $\dfrac{2T_t}{\pi R^3}$ values directly. Equation (3) was then used to obtain τ_R. Equation (2) also applies at $r = R$; thus, it can be written as

$$\dot{\gamma}_{aR} = \dot{\gamma}_R(\tau_R) + \frac{2U_S(\tau_R)}{H} \tag{4}$$

Yilmazer and Kalyon[5] generalized this method by using experiments at more than two gap heights, which provided better accuracy and showed that, if plots of $\dot{\gamma}_{aR}$ versus $1/H$ are drawn at constant τ_R, then straight lines are obtained according to eq. (4). The extrapolated intercepts are equal to $\dot{\gamma}_R(\tau_R)$ (i.e., the true shear rate at the edge), and the slopes are equal to $2U_S(\tau_R)$.

The true viscosity η can then be calculated by dividing the shear stress at the edge of the disk by the true shear rate at the edge of the disk:

$$\eta = \frac{\tau_R}{\dot{\gamma}_R} \tag{5}$$

RESULTS AND DISCUSSION

Slip Velocity

Figures 2 and 3 show the shear stress at the edge of the disk τ_R versus the apparent shear rate, $\dot{\gamma}_{aR}$, for representative systems without and with slip

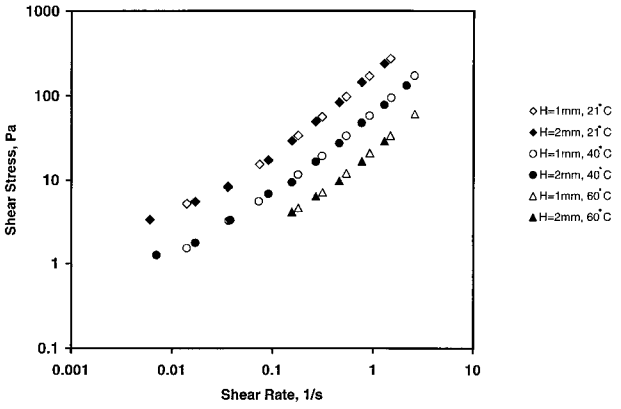

Figure 2 Shear stress at the edge of the disk (τ_R) versus the apparent shear rate, $\dot{\gamma}_{aR}$ for 50% aluminum (10.40 μm) at various temperatures and gap heights.

effects, respectively. As seen in Figure 2, in this case, the samples do not show slip effects because data of τ_R versus $\dot{\gamma}_{aR}$ are independent of the gap height at each temperature. However, in some cases, especially at concentrations very close to the maximum packing fraction of the particles, the shear stress values increased with increasing gap separation at a constant shear rate. This type of behavior represented in Figure 3 is thus indicative of the presence of wall slip in these experiments.

It was not possible to continue the parallel disk measurements above the shear rate range shown in the figures, because above these ranges the samples showed visible signs of fracture during steady shear flow. Table II shows the conditions in which materials showed slip at the walls of the viscometer.

In Figure 4, the apparent shear rate versus the reciprocal height data at constant τ_R, are shown for the system indicated in Figure 3. Data points fall reasonably well on the regression lines drawn through the points confirming the validity of eq. (4).

The slip velocity values in parallel disk torsional flow experiments calculated using the slopes as implied by eq. (4) versus the shear stress data of the suspensions at various temperatures are shown in Figure 5–9 in a logarithmic form. At a given shear stress value, the wall slip velocity increases with increasing temperature. The slip velocity, U_S, versus shear stress at the edge, τ_R, behavior follows a linear relationship such as

$$U_S = a \cdot \tau_R \tag{6}$$

where "a" is the temperature-dependent coefficient. The slopes of the lines in Figures 5–9 are equal to 1, as implied by the logarithmic form of eq. (6). The values of "a" for different materials at various filler fractions obtained from these lines and eq. (6) are shown in Table III.

Slip Layer Thickness

The slip-aided flow of the suspension takes place by "apparent slip" through the formation of a thin, liquid-rich layer at the wall thickness δ, allowing the suspension to slide through. This layer is referred to as the slip layer thickness in the context of apparent slip mechanism. The slip layer thickness can be calculated from eq. (7) or eq. (8).[5]

$$\delta = \frac{U_S \eta_S}{\tau_R} \tag{7}$$

or

$$\delta = a\,\eta_S \tag{8}$$

where η_S is the viscosity of the suspending liquid. The slip layer thickness for each material at different temperatures is shown in Table III. The values show that, in most cases, the slip layer thickness is independent of temperature for a particular filler. However, the suspension with 50% glass beads (150 μm) shows some dependence on the temperature at 60°C. This may be due to the settling of the particles at higher temperatures. If the slip layer thickness is

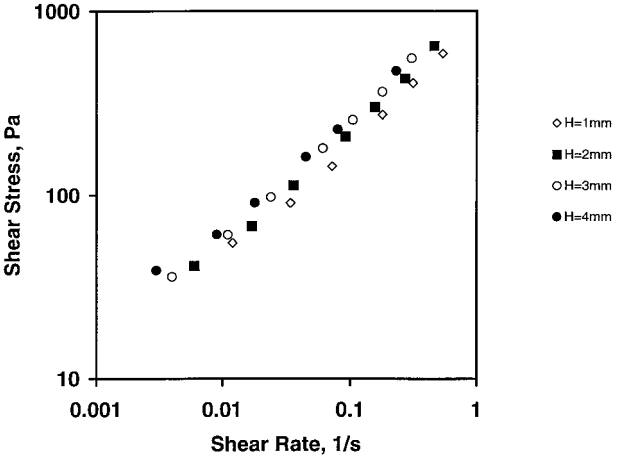

Figure 3 Shear stress at the edge of the disk (τ_R) versus the apparent shear rate, $\dot{\gamma}_{aR}$ for 63% glass beads (45.94 μm) at 21°C at various gap heights.

Table II Slip Effect Conditions

Material	Temperature (°C)	Packing Fraction [ϕ (%)]				
		30	40	50	58	63
AL (5.03 μm)	21	No slip	No slip	No slip		
	40	No slip	No slip	No slip	—	—
	60	No slip	No slip	No slip		
AL (10.4 μm)	21	No slip	No slip	No slip		Slip
	40	No slip	No slip	No slip	—	Slip
	60	No slip	No slip	No slip		Slip
GB (45.94 μm)	21					Slip
	40	—	—	—	—	Slip
	60					Slip
GB (150.0 μm)	21			No slip	Slip	Slip
	40	—	—	Slip	Slip	Slip
	60			Slip	Slip	Slip

AL, aluminum; GB, glass beads.

independent of temperature, eqs. (6) and (8) can be rewritten as[13]

$$U_S(\tau_R, T) = \left[\frac{\delta}{\eta_S(T)}\right] \cdot \tau_R \tag{9}$$

where

$$\delta = a(T)\eta_S(T) \tag{10}$$

These equations show that, at a constant δ, $\eta_S(T)$ and $a(T)$ are inversely related and if $\eta_S(T)$ decreases with increasing temperature, $a(T)$ will increase.

Overall, the slip velocity results indicate that the viscosity of the binder of the concentrated suspension significantly affects the slip behavior of the suspension, and a smaller binder viscosity gives rise to a greater wall slip velocity. Thus, increasing temperature for a given binder increases the wall slip velocity.

Effects of Particle Size and Volume Fraction of Solids on the Slip Layer Thickness

The data given in Table III show that the slip layer thickness increases with increasing size of the particles. The slip layer seems to be a fraction

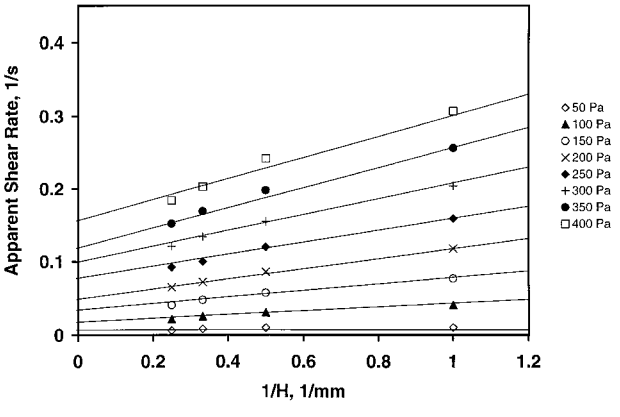

Figure 4 Apparent shear rate, $\dot{\gamma}_{aR}$ versus $1/H$ for 63% glass beads (45.94 μm) at 21°C. (Shear stress values are indicated.)

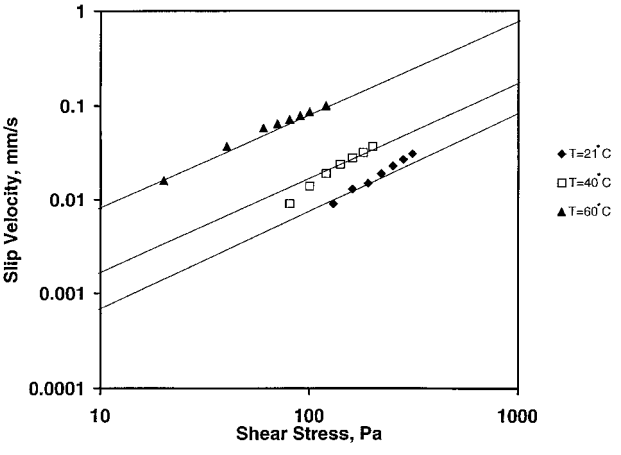

Figure 5 Slip velocity versus shear stress at different temperatures for 63% aluminum (10.40 μm).

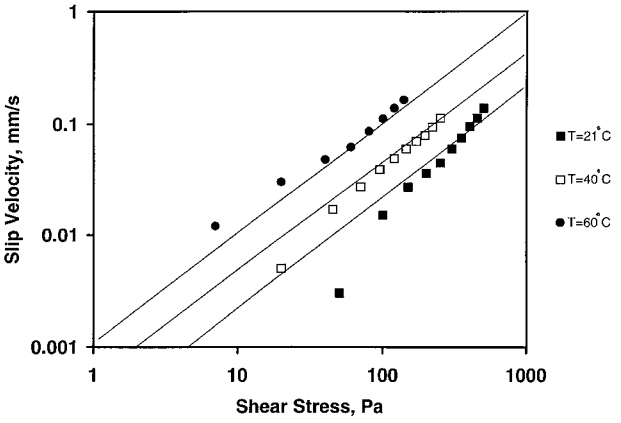

Figure 6 Slip velocity versus shear stress at different temperatures for 63% glass beads (45.94 μm).

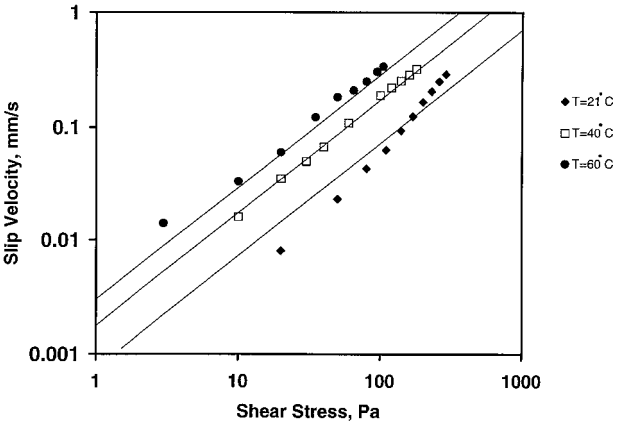

Figure 8 Slip velocity versus shear stress at different temperatures for 58% glass beads (150.0 μm).

of the particle size consistent with earlier findings on other types of concentrated suspensions.[5] To confirm this, δ/D_P values, i.e., the slip layer thickness divided with the average particle size, are also shown in Table III.

The δ/D_P values are plotted in Figure 10 as a function of ϕ/ϕ_m, the filler fraction normalized by the maximum filler fraction.

In the experiment of this study, suspensions with the smallest particles of aluminum (5.03 μm) did not show slip even at concentrations near their maximum packing fraction. In these suspensions with the smallest particles, δ, the slip layer thickness would be very small because D_P is small. If the slip layer thickness is comparable with the height of surface irregularities, then slip would not develop as observed herein. It is well known that, to prevent slip at the wall, roughened wall surfaces are used.

In the present study, other suspensions exhibited slip at the wall at high concentrations close to their maximum packing fraction. In this analysis, it is difficult to pinpoint the exact filler concentration at which the slip phenomenon starts. However, slip does not take place at low values of ϕ/ϕ_m. For the cases in which slip does take place, it seems that δ/D_P is insensitive to ϕ/ϕ_m, i.e., the slip layer, δ, is proportional to the particle size, but is relatively independent of the normalized filler fraction, ϕ/ϕ_m, and temperature.

The average value of δ/D_P is 0.037 for the glass beads and 0.071 for the aluminum at various values of temperature and ϕ/ϕ_m.

A δ/D_P value of 0.148 was reported in ref. 5 for a system that contained 60% by volume of ammonium sulfate particles (average size: 23 μm) in a polybutadiene acrylonitrile acrylic acid terpoly-

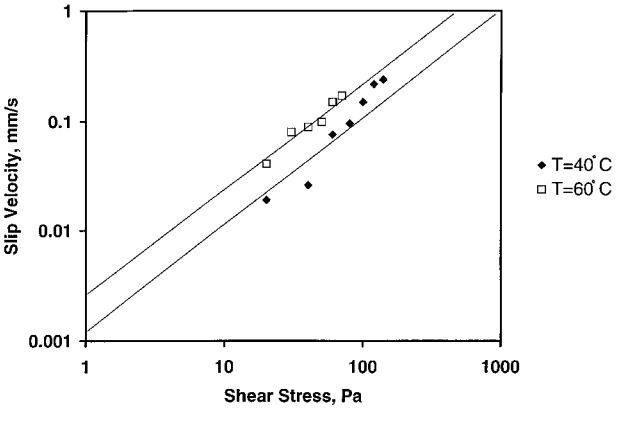

Figure 7 Slip velocity versus shear stress at different temperatures for 50% glass beads (150.0 μm).

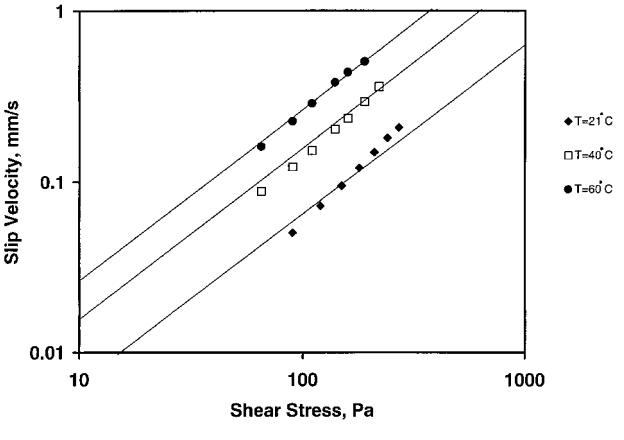

Figure 9 Slip velocity versus shear stress at different temperatures for 63% glass beads (150.0 μm).

Table III Slip Layer Thickness "δ" and "*a*" Values Obtained from Eqs. (7) and (6), Respectively

Material	Volume Fraction (ϕ)	a (μm/Pa · s)			δ (μm)			δ/D_P		
		T = 21°C	T = 40°C	T = 60°C	T = 21°C	T = 40°C	T = 60°C	T = 21°C	T = 40°C	T = 60°C
AL (5.03 μm)	0–0.5	0.00	0.00	0.00	No slip	No slip	No slip	—	—	—
AL (10.40 μm)	0–0.5	0.00	0.00	0.00	No slip	No slip	No slip	—	—	—
AL (10.40 μm)	0.63	0.088	0.180	0.51	0.74	0.73	0.75	0.071	0.070	0.072
GB (45.94 μm)	0.63	0.194	0.389	1.09	1.63	1.58	1.61	0.035	0.034	0.035
GB (150.00 μm)	0.50	0.00	1.348	2.34	No slip	5.49	3.44	—	0.037	0.023
GB (150.00 μm)	0.58	0.776	1.580	4.46	6.49	6.45	6.56	0.043	0.043	0.044
GB (150.00 μm)	0.63	0.672	1.390	1.47	5.63	5.66	5.70	0.038	0.038	0.038

AL, aluminum; GB, glass beads.

Figure 10 (Slip layer thickness/average particle diameter) δ/D_P versus (filler fraction/maximum packing fraction) ϕ/ϕ_m for the suspensions at different temperatures. GB, glass beads; AL, aluminum.

mer (viscosity 37 Pa s). Although this value is in the same order of magnitude as the results of the present study, further comparison is not attempted, because surface roughness are not known for both of the cases.

CONCLUSIONS

Flow behavior of highly filled suspensions above 30% by volume were characterized using parallel disk torsional viscometry and, for the first time, the effects of particle size, volume fraction, solid particle type and temperature on the slip velocity, and slip layer thickness were investigated by using multiple gap separations. In most cases, the flow of these highly filled suspensions was strongly affected by slip at the wall. Slip velocity was found to vary linearly with shear stress at the wall. Slip velocity values increased with increasing temperature. The increase of slip velocity with increasing temperature is principally related to the decrease of the shear viscosity of the binder. Slip layer thickness was found to increase proportionally with increasing size of the particles and, in most cases, it was independent of temperature. The plot of δ/D_P versus ϕ/ϕ_m showed that, up to a certain value of ϕ/ϕ_m, slip layer thickness is 0 (no slip), but it suddenly increases and remains relatively independent of

ϕ/ϕ_m for various temperatures and particle sizes for a given type of solid particle material.

NOMENCLATURE

a	temperature-dependent coefficient for slip layer thickness (mm Pa^{-1} s^{-1})
D_P	average diameter of particle (μm)
H	gap height (mm)
r	radial distance from the center of the disk (mm)
R	radius of the disk (mm)
T	temperature (K)
T_t	torque required to rotate the disk (N · m or dyne · mm)
U_S	slip velocity (mm s^{-1})
δ	slip layer thickness (mm)
$\dot{\gamma}$	shear rate experienced by the fluid (s^{-1})
$\dot{\gamma}_{aR}$	apparent shear rate at the edge of the disk (s^{-1})
Ω	angular velocity of the rotating disk (rps)
η	true viscosity of the suspension (Pa · s)
η_s	viscosity of the suspending liquid (Pa · s)
τ	shear stress experienced by the fluid (Pa)
τ_R	shear stress at the edge of the disk (Pa)
ϕ	volume fraction of the particles
ϕ_m	maximum packing fraction of the particles

REFERENCES

1. D. J. Jeffrey and A. Acrivos, *AlChE J.,* **22,** 417 (1976).
2. J. Mewis and A. J. B. Spaull, *Adv. Colloid Interface Sci.,* **6,** 173 (1976).
3. L. Hoffman, *J. Rheol.,* **36,** 947 (1992).
4. A. Barnes, *J. Rheol.,* **33,** 329 (1989).
5. U. Yilmazer and D. M. Kalyon, *J. Rheol.,* **33,** 1197 (1989).
6. H. Boersma, P. J. M. Baets, J. Laven, and H. N. Stein, *J. Rheol.,* **35,** 1093 (1991).
7. D. M. Kalyon, P. Yaras, B. Aral, and U. Yilmazer, *J. Rheol.,* **37,** 35 (1993).
8. R. Buscall, J. I. McGowan, and A. J. Morton-Jones, *J. Rheol.,* **37,** 621 (1993).
9. G. Menning, *Kunststoffe,* **74,** 296 (1984).
10. V. Vand, *J. Phys. Colloid Chem.,* **52,** 277 (1948).
11. A. Yoshimura and R. K. Prud'homme, *J. Rheol.,* **32,** 53 (1988).
12. M. Mooney, *J. Rheol.,* **2,** 210 (1931).
13. B. Aral and D. M. Kalyon, *J. Rheol.,* **38,** 957 (1994).